


Generalized Skyrme random-phase approximation for nuclear resonances: Different trends for electric and magnetic modes

J. Speth¹, P.-G. Reinhard², V. Tselyaev^{3,*} and N. Lyutorovich³

¹*Institut für Kernphysik, Forschungszentrum Jülich, D-52425 Jülich, Germany*

²*Institut für Theoretische Physik II, Universität Erlangen-Nürnberg, D-91058 Erlangen, Germany*

³*St. Petersburg State University, St. Petersburg 199034, Russia*

 (Received 9 January 2020; revised 1 April 2020; accepted 10 November 2020; published 30 November 2020)

We discuss major differences between electric and magnetic excitations in nuclei appearing in self-consistent calculations based on Skyrme energy-density functionals (EDFs). For this we calculate collective low- and high-lying electric and magnetic excitations in ^{208}Pb within a self-consistent Skyrme EDF approach using the random-phase approximation (RPA) and a more sophisticated particle-hole plus phonon-coupling model, coined the time-blocking approximation (TBA). Tools of analysis are Landau-Migdal parameters for bulk properties and the RPA and TBA results for finite nuclei. We show that the interplay between the effective mass and the effective particle-hole interaction, well known in the Landau-Migdal theory, renders the final results rather independent of the effective mass by virtue of the “backflow effect.” It explains the success of self-consistent calculations of electric transitions in such approaches. This effect, however, is absent in the magnetic case and leads to higher fluctuations in the results. It calls for further developments of the Skyrme functional in the spin channel.

DOI: [10.1103/PhysRevC.102.054332](https://doi.org/10.1103/PhysRevC.102.054332)

I. INTRODUCTION

This paper addresses the simultaneous description of nuclear electric and magnetic resonances by fully self-consistent methods based on Skyrme energy-density functionals (EDFs). It takes up the long known fact that electric resonances can be well described by Skyrme EDFs (for a review see [1]), whereas the first Skyrme EDF calculations of magnetic modes had already indicated a conflict when trying to cover both modes simultaneously [2,3]. We show here that this conflict can be understood already with simple fluid dynamical considerations for which we use here Landau-Migdal (LM) theory [4,5]. With the simple LM estimates in mind, we then investigate the collective low- and high-lying electric and magnetic resonances using the standard random-phase approximation (RPA), which is known to describe average excitation properties rather well [6]. This is augmented as a counter-check by the more sophisticated particle-hole plus phonon-coupling approach, coined time-blocking approximation (TBA), which improves the description of spectral fragmentation and widths [7,8].

Two different approaches have been successfully applied to calculation of nuclear resonance excitations. The traditionally most often used method employs a phenomenological single-particle model together with an effective residual interaction. A widely used and powerful version is Migdal’s theory of *finite Fermi systems* [4] based on Landau’s *theory of Fermi liquids* [5]. This approach has been applied extensively to a broad range of nuclei; for reviews see [9]. In the second

approach, one starts with an effective EDF which allows one to derive the single-particle model as well as the residual interaction. One of the most often used versions is the Skyrme-Hartree-Fock (SHF) approach [10–13]; for a review see [1]. Originally, it was designed as a model for the nuclear ground state [14]. But soon it was also applied to compute self-consistently collective excitation states, especially giant resonances. The parameters of the early Skyrme EDF were predominately adjusted to ground state properties, which does not *a priori* guarantee an appropriate particle-hole (ph) interaction. However, as incompressibility and symmetry energy are closely connected to the spin-independent isoscalar and isovector parts of the ph interaction, in general the theoretical results were not so bad. In later parametrizations, properties of excited states were also included, which improved the theoretical results compared to the data; see, e.g., [15,16]. The Skyrme EDF turned out to be flexible enough to reproduce all collective modes with natural parity. Most of the modern parameter sets use very similar values for the incompressibility K_∞ and symmetry energy a_{sym} . There is more variation in the choice of the effective mass m^* . As the effective mass has a heavy impact on the ph spectrum, it is very astonishing that the RPA results of giant resonances and also of low-lying collective states are, nonetheless, not very different. Let us take as examples the giant electric dipole resonances (GDR) and isoscalar monopole modes (GMR): For both modes, the position of the resonance peaks is found to be independent of the effective mass of a given parametrization [16,17]. However, if we choose a parameter set with a lower effective mass we increase the energy of ph excitations and one needs for the GDR a less repulsive isovector ph interaction to obtain similar theoretical results as before. Analogously, the isoscalar ph

*tselyaev@mail.ru

interaction has to become stronger in order to obtain similar results for the GMR. It seems that there exists a corrective mechanism which counterweights the spin independent isoscalar and isovector ph interaction in an appropriate way if the effective masses are changed. It is the main topic of our investigation to explore this fundamental mechanism for nuclear resonances with natural parity (electric modes) as well as with unnatural parity (magnetic modes).

It is instructive to learn from Landau-Migdal theory, which provides a compact and transparent way to quantify the residual ph interaction [4,5]. There, basic conservation laws establish a correlation between the parameters f_0 and f'_0 of the (spin-independent) isoscalar and isovector residual interaction with the incompressibility K_∞ and symmetry energy a_{sym} [4]:

$$f_0 = \frac{K_\infty}{6T_F} - \frac{m}{m^*}, \quad f'_0 = \frac{3a_{\text{sym}}}{T_F} - \frac{m}{m^*}, \quad (1a)$$

where

$$T_F = \frac{\hbar^2 k_F^2}{2m} \quad (1b)$$

is the kinetic energy at the Fermi surface. As we see from the formulas above: with decreasing effective masses the isoscalar ph interaction gets more attractive and the isovector ph interaction becomes less repulsive, thus correcting for the larger ph-energy spacing. Therefore, the spin-independent ph interactions in the LM approach depend, for given K_∞ and a_{sym} , on the effective mass m^*/m . (These relations are derived in nuclear matter and hold bulk parameters of Migdal's ph interaction, also coined "inner" parameters [9].) The interplay between effective mass and interaction strength is a feature similar to the *backflow* of quasiparticles in condensed matter [18]. Such correlations hold also in EDF approaches, which means that independently of a given effective mass it is sufficient to use the appropriate incompressibility and symmetry energy in order to reproduce isovector as well as isoscalar electric (i.e., natural parity) resonances. This explains, e.g., the outcome of the first self-consistent calculation of electric resonances with the Skyrme interactions SI and SII in [19]. The results for the isovector dipole resonances were acceptable (with the exception of the splitting in ^{208}Pb) while the isoscalar monopole modes were predicted too high compared to the later experimental values because a too large incompressibility was inherent in the early Skyrme forces [20].

The major goal of our paper is to investigate such correlations also for the spin-independent part of the ph interaction in self-consistent calculations in the framework of Skyrme EDFs. For this purpose, we present a large body of theoretical results obtained with a variety of Skyrme parametrizations with different effective masses. To support the results from a formal side, we derive the Landau-Migdal parameter as functions of the effective mass. The parameters f_0 and f'_0 which determine the electric transitions show the expected behavior: With decreasing effective mass the spin-independent isoscalar parameter f_0 becomes more attractive and the corresponding isovector parameter f'_0 less repulsive.

The situation is more involved at the side of magnetic modes. Unfortunately, there are no spin magnetic *bulk*

properties known which are directly related to the spin-dependent parameters of EDFs, and the Landau-Migdal parameters g_0 and g'_0 respectively. Moreover, there exists only one truly collective spin mode, namely the Gamow-Teller (GT) resonance in neutron rich nuclei, which is related to the spin-isospin part of the residual ph interaction. Therefore, the parameters which are most relevant for the spin-dependent part of the ph interaction of the existing parametrizations were not yet adjusted to experimental properties with the exception of the two-body spin-orbit interaction. Bell and Skyrme introduced already more than 50 years ago a two-body spin-orbit term into the original ansatz in order to reproduce the single particle (sp) spin-orbit splitting [21]. Van Giai and Sagawa [22] modified two Skyrme parametrizations where they considered the spin-dependent LM parameters g_0 and g'_0 as additional constraints and calculated GT states in some doubly magic nuclei. The method of choice to learn more about nuclear interactions in the spin channel is then to look at magnetic excitation spectra in nuclei. Earlier studies used mixed models where the RPA residual interaction is modeled explicitly in addition to the underlying single-particle model; see, e.g., [23–26]. Fully self-consistent calculations of magnetic excitations are very scarce. They came up only recently [2,3,27,28] and point toward insufficiencies of the Skyrme EDF as given. In the survey [28], the spin-relevant parameters of the Skyrme EDF were modified to reproduce the experimental data, which amounts to a substantial readjustment of the LM parameters g_0 , g'_0 . These parameters do not show any corrective correlations as a function of the effective mass. In fact, the interaction parameters show just the opposite behavior: both parameters increase with decreasing effective mass. For completeness, we mention in passing that two distinctively different kinds of $M1$ states exist in deformed nuclei: The spin-flip resonances (as discussed here) and the *orbital* $M1$ states. The latter ones are located below the spin-flip states and are driven by the spin-independent ph interaction [29–31]. The spin-flip $M1$ states in well deformed nuclei show a remarked double hump-structure as predicted in Refs. [32,33] and are further analyzed in Ref. [34].

The aim of this paper is, as mentioned before, to unravel the success of conventional Skyrme EDF for the natural parity (also called electric) collective resonances and the failure in the spin channel. We use as a tool the trends of LM parameters with effective mass. We start with the well settled and well working case of the electric modes where we find that the "backflow effect" on the ph interaction is the key to success. Then we apply the same strategy to LM parameters in the spin channel. In Sec. II, we give a short review of the Skyrme approach. In Sec. III we present the relevant formulas of the Landau-Migdal approach where we especially emphasize the connection of the LM parameter with nuclear matter properties. In this connection, we analyze the functional behavior of the spin-dependent and spin-independent LM parameters on the effective mass. Section IV contains the main result of our investigation. First, we compare RPA and TBA results of electric giant resonances with unperturbed ph energies for various Skyrme parametrizations. In the second part, we show the corresponding results for the magnetic

states, using as example the 1^+ in ^{208}Pb . Finally, we summarize and discuss our results in Sec. V. In Appendix A, we discuss the density dependence of f_0 and f'_0 , which is crucial in the LM theory. As a supplement to the section on giant resonances, we present in Appendix B RPA results for low-lying collective states. Appendices D and E contain the known formulas expressing the nuclear matter properties and the LM parameters in terms of the parameters of the Skyrme EDF.

II. THE SKYRME ENERGY FUNCTIONAL

The Skyrme energy functional consists of kinetic energy, Coulomb energy, pairing energy, and, as key entry, the Skyrme interaction energy. This is well documented in several reviews; see, e.g., [1,35]. We recall here just the core piece as far as is needed in following. The Skyrme interaction energy is formulated in terms of a few nuclear densities and currents, such as density ρ_T , kinetic density τ_T , spin-orbit density \vec{J}_T , spin-tensor density \mathbb{J}_T , current \vec{j}_T , spin density \vec{s}_T , and spin kinetic density, where the index T stands for isospin ($T = 0$ or 1). It reads, in commonly used form,

$$\mathcal{E}_{\text{Sk}} = \sum_{T=0,1} (\mathcal{E}_T^{\text{even}} + \mathcal{E}_T^{\text{odd}}), \quad (2a)$$

$$\mathcal{E}_T^{\text{even}} = C_T^\rho(\rho_0) \rho_T^2 + C_T^{\Delta\rho} \rho_T \Delta\rho_T + C_T^{\tau} \rho_T \tau_T + C_T^{\nabla J} \rho_T \nabla \cdot \vec{J}_T (+ C_T^{\mathbb{J}} \mathbb{J}_T^2), \quad (2b)$$

$$\mathcal{E}_T^{\text{odd}} = C_T^s(\rho_0) \vec{s}_T^2 + C_T^{\Delta s} \vec{s}_T \cdot \Delta \vec{s}_T + C_T^j \vec{j}_T^2 + C_T^{\nabla j} \vec{s}_T \cdot \nabla \times \vec{j}_T (+ C_T^{sT} \vec{s}_T \cdot \vec{\tau}_T). \quad (2c)$$

The terms employing the tensor spin-orbit densities are written in parentheses to indicate that these terms are ignored in the majority of published Skyrme parametrizations. Only the time-even part $\mathcal{E}_T^{\text{even}}$ is relevant for ground states of even-even nuclei. Time-odd nuclei and magnetic excitations are sensitive also to the time-odd part $\mathcal{E}_T^{\text{odd}}$. The parameters C_T^{type} for each term in the time-even part are adjusted independently, usually to a carefully chosen set of empirical data [1,35]. A couple of different options are conceivable for the parameters of the time-odd terms, which has consequences for the description of magnetic modes. This will be discussed in Sec. IV C.

The original formulation of the SHF method was based on the concept of an effective interaction, coined the Skyrme force [10]. Modern treatments of SHF, however, start from a Skyrme energy-density functional as shown above. Nonetheless, the Skyrme force was the original motivation to develop the Skyrme functional and, being a zero-range interaction, displays an obvious similarity to the Landau-Migdal force. Its interaction part without spin-orbit and Coulomb terms has the form

$$E_{\text{Sk}}^{\text{int}} = E_{\text{Sk,dens}}^{\text{int}} + E_{\text{Sk,grad}}^{\text{int}}, \quad (3a)$$

$$E_{\text{Sk,dens}}^{\text{int}} = \langle \Phi | t_0 (1 + x_0 \hat{P}_\sigma) \delta(\mathbf{r}_{12}) + \frac{t_3}{6} (1 + x_3 \hat{P}_\sigma) \rho^\alpha(\mathbf{r}_1) \delta(\mathbf{r}_{12}) | \Phi \rangle, \quad (3b)$$

$$E_{\text{Sk,grad}}^{\text{int}} = \langle \Phi | \frac{t_1}{2} (1 + x_1 \hat{P}_\sigma) (\hat{\mathbf{k}}^{\dagger 2} \delta(\mathbf{r}_{12}) + \delta(\mathbf{r}_{12}) \hat{\mathbf{k}}^2) + t_2 (1 + x_2 \hat{P}_\sigma) \hat{\mathbf{k}}^\dagger \cdot \delta(\mathbf{r}_{12}) \hat{\mathbf{k}} | \Phi \rangle, \quad (3c)$$

where $\mathbf{r}_{12} = \mathbf{r}_1 - \mathbf{r}_2$ and $\hat{P}_\sigma = \frac{1}{2}(1 + \hat{\sigma}_1 \hat{\sigma}_2)$ is the spin-exchange operator. The $\hat{\mathbf{k}}$ stand for the momentum operators (see [1]).

The Skyrme interaction (3) is not to be mixed with the residual interaction for computing excitation properties within RPA, called henceforth ph interaction. This residual interaction is deduced as second functional derivative of the Skyrme energy functional (2) [36] with respect to the local densities and currents it contains. As the functional (2) is composed of contact terms, the RPA residual interaction is a zero-range interaction. In that respect, it is very similar to the Landau-Migdal interaction, a feature which motivates a discussion of Skyrme RPA excitations in terms of the LM parameters as we do here.

The Skyrme functional contains kinetic terms, which leads to an effective nucleon mass m^* which differs from the bare mass m in the nuclear interior. This has consequences for many time-odd observables. For example, the current operator \hat{j}_q fails to satisfy the continuity equations if $m^* \neq m$. The nontrivial kinetic terms in the mean-field Hamiltonian call for a dynamical correction which reads [37]

$$\hat{j}_{\text{eff},q} = \hat{j}_q + \frac{m_q}{\hbar^2} (2b_1 [\rho_{\bar{q}} \hat{j}_q - \rho_q \hat{j}_{\bar{q}}] + b_4 [\rho_{\bar{q}} \nabla \times \hat{\sigma}_q - \rho_q \nabla \times \hat{\sigma}_{\bar{q}}]), \quad (4)$$

where q denotes proton or neutron, \bar{q} the nucleon with opposite isospin, and the coefficients b_1 and b_4 are defined in Ref. [36]. This correction is crucial, e.g., in the computation of transition strengths for giant resonances [6]. It exemplifies the backflow effect known from the theory of Fermi liquids [38]. The same correction is also required for the magnetic current [39]. We will see below that a similar backflow-like correction appears also for the residual interaction in RPA.

III. LANDAU-MIGDAL THEORY

The Landau-Migdal theory of excitations in fermionic systems was developed originally in the context of Fermi fluids [40–42] and extended later to finite nuclei [4]. The LM ph interaction is restricted to the Fermi surface, where it depends only on the angle between the momenta \mathbf{p} and \mathbf{p}' of the 1ph states before and after the collision. The ph interaction in momentum space is a function $F^{\text{ph}}(\mathbf{p}, \mathbf{p}')$ times spin and isospin operators. The momentum dependence can be expanded in terms of Legendre polynomials in the dimensionless combination $\mathbf{p} \cdot \mathbf{p}' / |\mathbf{p}| |\mathbf{p}'|$ [40–42]. The coefficients of this expansion are called LM parameters. The leading order ($l = 0$) of the Legendre polynomial is a constant which gives rise in \mathbf{r} -space to a delta function [$F^{\text{ph}}(1, 2) = \delta(\mathbf{r}_{12})$] similar to the leading term in the Skyrme interaction. The term next to leading order ($l = 1$) is proportional to $(\mathbf{p} \cdot \mathbf{p}')$. To deal better with the finite size of the nuclei, one often introduces density-dependent LM

parameters in the following way [4]:

$$f(\rho) = f^{\text{ex}} + (f^{\text{in}} - f^{\text{ex}}) \frac{\rho_0(r)}{\rho_0(0)},$$

where f^{ex} stands for the exterior region of the nucleus and f^{in} for the interior. However, the density dependence of the Skyrme ph interaction differs from that form, which would require a discussion of its own [43]. Thus we concentrate on the interior region, the nuclear bulk properties, and drop the upper index “in” in the following.

A. Dimensionless Landau-Migdal parameters

The expansion parameters have the same dimension as the interaction, namely energy \times length³, which varies strongly with system size. To obtain a dimensionless measure of interaction strength, it is customary to single out a normalization factor having this dimension. A natural measure of length³ is the inverse of bulk density ρ_0 . Thus Migdal uses as normalization factor the derivative $C_0^{(\text{Migdal})} = d\epsilon_F/d\rho_0 = \pi^2 \hbar^2 / (mk_F) \approx 300 \text{ MeV fm}^3$, which applies to models using bare nucleon mass m [4]. Landau *et al.* take a similar normalization factor; however, it is half of Migdal’s, and they use the effective nucleon mass m^* in the definition [5]. This amounts to parametrizing the RPA interaction in terms of LM parameters F_l, G_l as

$$F^{\text{ph}}(\mathbf{p}, \mathbf{p}') = C_0^* \sum_l P_l \left(\frac{\mathbf{p} \cdot \mathbf{p}'}{k_F^2} \right) [F_l + F_l' \tau_1 \cdot \tau_2 + G_l \sigma_1 \cdot \sigma_2 + G_l' \sigma_1 \cdot \sigma_2 \tau_1 \cdot \tau_2], \quad (5a)$$

$$C_0^* = \frac{\pi^2 \hbar^2}{2m^* k_F} \approx 150 \text{ MeV fm}^3 \times \frac{m}{m^*}. \quad (5b)$$

This normalization has the advantage that the condition for stable RPA modes becomes simply $F_0 > -1$ and it is most suited for self-consistent nuclear models where effective mass $m^* \neq m$ plays a role. Many publications in the context of the SHF model use this normalization. Still, Migdal’s definition using a fixed normalization factor is also often used, particularly in the empirical LM model. Thus we discuss both definitions. However, we want to avoid the trivial, but distracting, factor 2 in the comparison, and we use for that the normalization form

$$F^{\text{ph}}(\mathbf{p}, \mathbf{p}') = C_0 \sum_l P_l \left(\frac{\mathbf{p} \cdot \mathbf{p}'}{k_F^2} \right) [f_l + f_l' \tau_1 \cdot \tau_2 + g_l \sigma_1 \cdot \sigma_2 + g_l' \sigma_1 \cdot \sigma_2 \tau_1 \cdot \tau_2], \quad (6a)$$

$$C_0 = \frac{\pi^2 \hbar^2}{2mk_F} \approx 150 \text{ MeV fm}^3. \quad (6b)$$

Henceforth we call the choice (6) “bare-mass normalization” and the choice (5) “effective-mass normalization.” Each one of the two definitions has its advantages and disadvantages. The bare-mass normalization (6) produces a measure of strength of residual interaction term by term comparable across SHF parametrizations with different m^*/m . The effective-mass normalization (5) produces comparable effects of the residual interaction (stability condition, excitation

TABLE I. The two forms of LM parameters (6) and (5) and their relation to nuclear matter properties. Upper block: definition of LM parameters in terms of NMP. Lower block: NMP computed from LM parameters. The kinetic energies T_F and T_F^* are defined in Eq. (7).

LM parameters		
Effective-mass normalization	Bare-mass normalization	
$F_0 = \frac{K_\infty}{6T_F^*} - 1$	$f_0 = \frac{m}{m^*} F_0 = \frac{K_\infty}{6T_F} - \frac{m}{m^*}$	
$F_0' = \frac{3a_{\text{sym}}}{T_F^*} - 1$	$f_0' = \frac{m}{m^*} F_0' = \frac{3a_{\text{sym}}}{T_F} - \frac{m}{m^*}$	
$F_1 = 3 \left(\frac{m^*}{m} - 1 \right)$	$f_1 = \frac{m}{m^*} F_1 = 3 \left(1 - \frac{m}{m^*} \right)$	
$F_1' = 3 \left((1 + \kappa_{\text{TRK}}) \frac{m^*}{m} - 1 \right)$	$f_1' = \frac{m}{m^*} F_1' = 3 \left(1 + \kappa_{\text{TRK}} - \frac{m}{m^*} \right)$	
LM parameters		
NMP	Consistent norm.	Fixed norm.
$\frac{K_\infty}{6} =$	$T_F^* (1 + F_0)$	$T_F \left(\frac{m}{m^*} + f_0 \right)$
$\frac{m}{m^*} =$	$\frac{1}{1 + \frac{F_1}{3}}$	$1 - \frac{f_1}{3}$
$3a_{\text{sym}} =$	$T_F^* (1 + F_0')$	$T_F \left(\frac{m}{m^*} + f_0' \right)$
$1 + \kappa_{\text{TRK}} =$	$\frac{m}{m^*} \left(1 + \frac{F_1'}{3} \right)$	$\frac{m}{m^*} + \frac{f_1'}{3}$

energies). The reason is that different interaction strengths are required to compensate for the impact of different m^*/m , similarly as in the backflow effect [18]; see Eq. (4).

B. Relation to nuclear matter properties

First, we look at nuclear matter properties (NMP), which provide a unique characterization of the basic nuclear response properties in the volume: incompressibility K_∞ , effective mass m^*/m , symmetry energy a_{sym} , and Thomas-Reiche-Kuhn (TRK) sum rule enhancement κ_{TRK} . The first two are isoscalar response properties and the second two are isovector properties. The κ_{TRK} is a way to parametrize the isovector effective mass [1]. All four are the response properties in the excitations channels with natural parity. The NMP for spin modes are not nearly that well developed, particularly because the data basis on magnetic excitations is not strong enough to support unambiguous extrapolation to bulk. Thus we concentrate first on the group of natural parity modes. In many of the expressions for NMP there appears the (effective) nucleon mass, frequently in the formula for the kinetic energy T_F of bulk matter. To simplify notations, we introduce for it the abbreviations

$$T_F = \frac{\hbar^2 k_F^2}{2m}, \quad T_F^* = \frac{\hbar^2 k_F^2}{2m^*} = \frac{m}{m^*} T_F. \quad (7)$$

Columns 1 and 2 in the upper block of Table I list the LM parameters in effective-mass and bare-mass normalization together with their relations to NMP. The parameters in

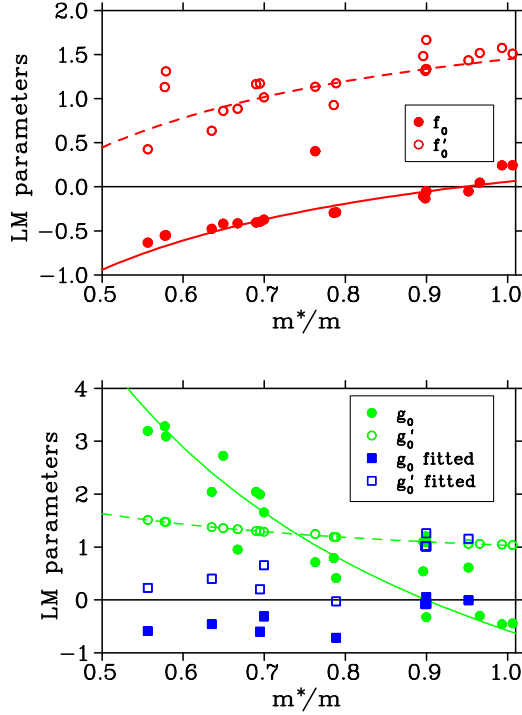


FIG. 1. Dependence of the LM parameters on the effective mass m^*/m . Upper panel: f_0 (filled red circles), f'_0 (open red circles) derived from the collection of the most widely used Skyrme parametrizations given in Table I of [28]. The lines indicate the trends $a + bm^*/m$ of f_0 (solid line) and f'_0 (dashed line), computed with the NMP of SV-bas (Table II) except for m^*/m which is varied. Lower panel: g_0 (filled green circles) and g'_0 (open green circles) for the same Skyrme parametrizations. The lines indicate again the trends $a + bm^*/m$ (solid line for g_0 , dashed line for g'_0). Also shown are the adjusted LM spin parameters which reproduce the magnetic dipole states in ^{208}Pb (g_0 as filled blue squares, g'_0 as open blue squares) for the corresponding Skyrme parametrizations taken from [28].

effective-mass normalization (column 1) demonstrate nicely the interplay between mean field (terms with the leading contribution “1”) and the residual interaction (terms with F ’s). With bare-mass normalization, the terms representing the mean field are in most cases proportional to m/m^* , which takes into account that self-consistent models can stretch or squeeze the level spacing and the residual interaction thus has to work against the modified level density, similar to the backflow effect, Eq. (4), for currents. The lower block shows, in turn, how NMP are computed from LM parameters. Again, the place where the effective mass enters makes the crucial difference between bare-mass normalization and effective-mass normalization. Particularly noteworthy are the entries for f_1 and f'_1 , or F_1 and F'_1 respectively. These show that self-consistent models establish an intimate connection between these first-order parameters and effective masses m/m^* and κ_{TRK} . One is not allowed to change one without consistently modifying the other. This counter-play is also reflected in the backflow correction, Eq. (4), for flow observables.

The dimensionless LM parameters allow also one to express the stability conditions for excitations modes. These

are $F_0^{(l)} > -1$ for effective-mass normalization or $\frac{m^*}{m} f_0^{(l)} > -1$ for bare-mass normalization, and similarly $F_1^{(l)} > -3$ or $\frac{m^*}{m} f_1^{(l)} > -3$ for $l = 1$ [where the compact upper index (l) means that this holds for F as well as for F' type parameters]. The stability conditions look more natural for effective-mass normalization while one has first to undo the m/m^* factor in case of bare-mass normalization.

As argued above, the parameters f_0, f'_0 , defined with bare-mass normalization, represent directly the strength of the residual interaction. The first two lines of Table I show a clear dependence $f_0^{(l)} = c - m/m^*$, where c is some constant: The smaller m^* is, the stronger the isoscalar interaction and the weaker the isovector one, which is necessary to counterweight the lower level density at the Fermi surface (the “backflow effect” for the RPA interaction). The upper panel of Fig. 1 shows these trends for the natural-parity channel together with the values for $f_0^{(l)}$ from a representative set of well working Skyrme parametrizations. The results from the realistic parametrizations fit nicely to the analytic trend and so confirm the need to properly counterweight the level-spreading effect of the effective mass.

For completeness, we show in Table II the NMP and corresponding LM parameters for a selection of Skyrme parametrizations with systematically varied NMP [16,44]. The detailed expressions of the LM parameters in terms of the parameters of the Skyrme interaction (3) are given in Appendix E.

C. The spin channel

Now we turn to the spin channel, and we will see that the case is dramatically different. A first problem is that we do not have well established NMP for spin response and that spin modes in finite nuclei are not as prominent as giant resonances of natural parity. Both together leave the empirical calibration of the residual interaction in the spin channel an open problem [28]. Second, the spin channel in many mean-field models is determined once the natural-parity response is fixed. For example, relativistic mean-field models tie spin properties and kinetic properties closely together [45]. This may not be beneficial if it turns out that the “predictions” thus obtained are wrong. That is the aspect which we will address here for the case of the SHF model.

The spin properties in the Skyrme EDFs are not uniquely fixed. These leaves different options for their choice [46], which lead to rather different results for the LM parameters of G type:

- (1) One can understand SHF as stemming from the effective density-dependent zero-range interaction (3) which determines all spin terms from the given natural-parity partners and its NMP. This yields, by combining the formulas of Appendices D and E,

$$g_0 + g_1 = -(3 + 3\kappa_{\text{TRK}}) - \frac{3a_{\text{sym}} - 2\frac{B}{A}}{T_F} + \frac{26m}{5m^*}, \quad (8a)$$

$$g'_0 + g'_1 = \frac{B}{A} \frac{1}{T_F} + \frac{3}{5} \frac{m}{m^*}. \quad (8b)$$

TABLE II. Nuclear matter parameters for the Skyrme parametrizations used in this paper and the corresponding LM parameters in both normalizations.

EDF	m^*/m	K_∞ (MeV)	κ_{TRK}	a_{sym} (MeV)	F_0	F'_0	F_1	f_0	f'_0	f_1	G_0	G'_0	g_0	g'_0
SV-mas10	1.00	234	0.4	30	0.06	1.45	0.00	0.06	1.45	0.00	-0.58	1.03	-0.58	1.03
SV-bas	0.90	233	0.4	30	-0.05	1.20	-0.30	-0.05	1.34	-0.33	0.00	0.99	0.00	1.10
SV-kap00	0.90	233	0.0	30	-0.05	1.20	-0.30	-0.05	1.33	-0.34	1.08	0.99	1.20	1.10
SV-K218	0.90	218	0.4	30	-0.12	1.18	-0.30	-0.13	1.32	-0.34	0.02	0.99	0.02	1.10
SV-sym34	0.90	234	0.4	34	-0.04	1.50	-0.30	-0.05	1.67	-0.33	-0.29	0.99	-0.33	1.10
SV-mas07	0.70	234	0.4	30	-0.26	0.71	-0.90	-0.37	1.01	-1.29	1.16	0.90	1.65	1.29
SV-m64k6	0.64	241	0.6	27	-0.30	0.40	-1.09	-0.48	0.64	-1.72	1.30	0.87	2.04	1.38
SV-m56k6	0.56	255	0.6	27	-0.35	0.24	-1.33	-0.63	0.43	-2.39	1.78	0.84	3.19	1.51

- (2) Even when taking the viewpoint of option 1, most actual parametrizations drop the tensor spin-orbit terms (“tensor terms”) $\propto \vec{J}^2$ which are generated as partners of the kinetic terms in the force definition of the SHF functional. This yields the variant

$$g_0 = -(3 + 3\kappa_{\text{TRK}}) - \frac{3a_{\text{sym}} - 2\frac{B}{A}}{T_{\text{F}}} + \frac{26}{5} \frac{m}{m^*}, \quad (9a)$$

$$g'_0 = \frac{B}{A} \frac{1}{T_{\text{F}}} + \frac{3}{5} \frac{m}{m^*}, \quad (9b)$$

$$g_1 = 0, \quad (9c)$$

$$g'_1 = 0. \quad (9d)$$

- (3) One can dismiss the concept of a force and start from an EDF, in which case the spin terms are constrained only by the requirement of Galilean invariance, leaving a couple of terms open. These can be adjusted independently of the terms of natural parity and so allow for more flexible tuning of magnetic modes. This has been done, e.g., in [28]. No closed formula for the G parameters can be given here.
- (4) As in option 3, one can start from a Skyrme energy-density functional, but now freeze the spin terms by the requirement of “minimal Galilean invariance” which means to discard all spin terms which are not fixed by Galilean invariance [46]. This yields for the G parameters the trivial result

$$G_0 = 0, \quad G'_0 = 0, \quad G_1 = 0, \quad G'_1 = 0. \quad (10)$$

Let us first investigate the option 2, which assumes an underlying Skyrme force and thus predicts the properties in the spin channel from the known properties in the natural-parity channel. The LM parameters are thus given by Eqs. (9). The trend with m^* is of the form $g_0^{(l)} = a^{(l)} + b^{(l)}m/m^*$, where $a^{(l)}$ and $b^{(l)}$ are some constants. This looks similar to the trend for the $f_0^{(l)}$. The crucial difference is, however, that the mass dependence comes with a plus sign. The trend is visualized in the lower panel of Fig. 1. Note that the deviation of the open green circles from the dashed line is negligible because the first term in the right-hand side of Eq. (9b) is practically the same for all parametrizations. We see that the $g_0^{(l)}$ parameters increase with decreasing m^*/m , which goes the wrong way because it is counterproductive for compensating the decrease

of level density in the single-particle spectrum. The options 1 and 2 which treat the SHF model as an effective interaction are thus to be discarded for principle reasons.

This result has also been found in several places from studying magnetic excitations in finite nuclei; see, e.g., [3,28]. In [28], the spin parameters in the Skyrme functional had been adjusted freely to $M1$ modes in finite nuclei. This corresponds to option 3 in the above list. The resulting $g^{(l)}$ are shown as squares in Fig. 1. The g_0 stay close to zero for the parametrizations with $m^*/m \approx 1$. The g'_0 a bit larger, still being small. Both show a slight tendency to decrease with decreasing m^*/m , which is the expected trend. This empirical result allows also the option 4 for g_0 . This is not so clear for g'_0 . To be on the safe side, the option 3 turns out to be the recommended option.

IV. LANDAU-MIGDAL PARAMETERS AND RESONANCE EXCITATIONS IN ^{208}Pb

A. The random-phase approximation

In this section, we are going to investigate excitation properties in a finite nucleus, namely ^{208}Pb . The most often used method for calculating excitation properties in nuclear physics is the RPA and its various extended versions. There exist numerous different derivations which all lead to the same basic RPA equation [6]:

$$(\epsilon_{v_1} - \epsilon_{v_2} - \Omega_m)\chi_{v_1 v_2}^{(m)} = (n_{v_1} - n_{v_2}) \sum_{v_3 v_4} F_{v_1 v_4 v_2 v_3}^{\text{ph}} \chi_{v_3 v_4}^{(m)}. \quad (11)$$

The $\chi_{v_1 v_2}^{(m)}$ are the ph excitation amplitudes in the single-particle configuration space, F^{ph} is the ph interaction, ϵ_v are the sp energies, and Ω_m the excitation energies of the nucleus. There exist two different methods to determine the input data:

(I) The phenomenological shell-model approach where one starts with an empirically adjusted single-particle model and parametrizes the ph interaction. A very successful approach in this connection is the Landau-Migdal theory [4,47].

(II) The self-consistent approach where one starts with an effective EDF from which one derives the single-particle quantities as well as the ph interaction [36]. In this paper we discuss particularly Skyrme type EDFs.

There exist various extended versions of RPA which include configurations beyond 1ph, e.g., phonon coupling in the

TBA; for details see [7,8]. Most of these models employ again the basic ph interaction F^{ph} . Thus no new parameters have to be introduced.

The RPA equation (11) shows that there are two basic ingredients which determine at the end the excitation spectra: the 1ph energies $\epsilon_p - \epsilon_h$ and the ph interaction F^{ph} . The 1ph energies are determined with the ground state, which leaves little leeway for tuning. The ph interaction is exclusively seen in the excitations and most of their impact can be characterized in simple terms through the LM parameters, as done throughout this paper.

B. Giant resonances

We start with excitations of natural parity, also called electric modes. Their spectral distribution in a heavy nucleus as ^{208}Pb and in channels with low angular momentum L is dominated by one strong peak called a giant resonance. Most prominent are the isoscalar giant monopole resonance (GMR), the isoscalar giant quadrupole resonance (GQR), and the isovector giant dipole resonance (GDR). All three resonances can be characterized by one number, the resonance energy, which we will use now for looking at trends and relations to LM parameters. Figure 2 collects giant-resonance properties together with the leading LM parameters (upper panels) for a variety of Skyrme parametrizations with systematically varied NMP; see Table II. In order to check the impact of complex configurations beyond RPA, we compare resonance energies from RPA with those from TBA. The differences in the energies are small while the resonance width is significantly affected by the complex configurations in TBA [28,48,49]. At present, we focus on resonance energies and can ignore the small difference between RPA and TBA. Together with the resonance energies, we show also the average 1ph energies ϵ_{ph} (averaged over the 1ph spectrum weighted by the transition operator of each mode). The difference between ϵ_{ph} and the resonance energy provides a visualization of the impact of the ph interaction. It is obviously considerable: strongly attractive in the isoscalar modes [panels (c), (d), and (e) of Fig. 2] and strongly repulsive in the isovector modes [panels (a) and (b)]. Note that the Skyrme parametrizations are sorted in order of decreasing effective mass with $m^*/m = 1$ to the left and the lowest $m^*/m = 0.56$ to the right. It is obvious that the ϵ_{ph} increase while the resonance energies change comparatively little. The increase of ϵ_{ph} is largely compensated by a properly counteracting trend of the ph interaction. This trend can be nicely read off from the LM parameters shown in the upper panels. It is the same as shown already in Fig. 1, and we learn from the present figure that the trend $\propto c - m/m^*$ which is typical for the LM parameters in the natural parity channels is exactly what is needed to compensate for the dilution of 1ph spectra with decreasing effective mass.

Although the variations of resonance energies are small compared to the effects of the ph interaction, there is an important trend in them. It demonstrates the known intimate connection between NMP and resonance energies [16]: the giant monopole resonance (GMR) is related exclusively to the incompressibility K_∞ , the giant dipole resonance (GDR) to the sum rule enhancement κ_{TRK} , and the giant quadrupole

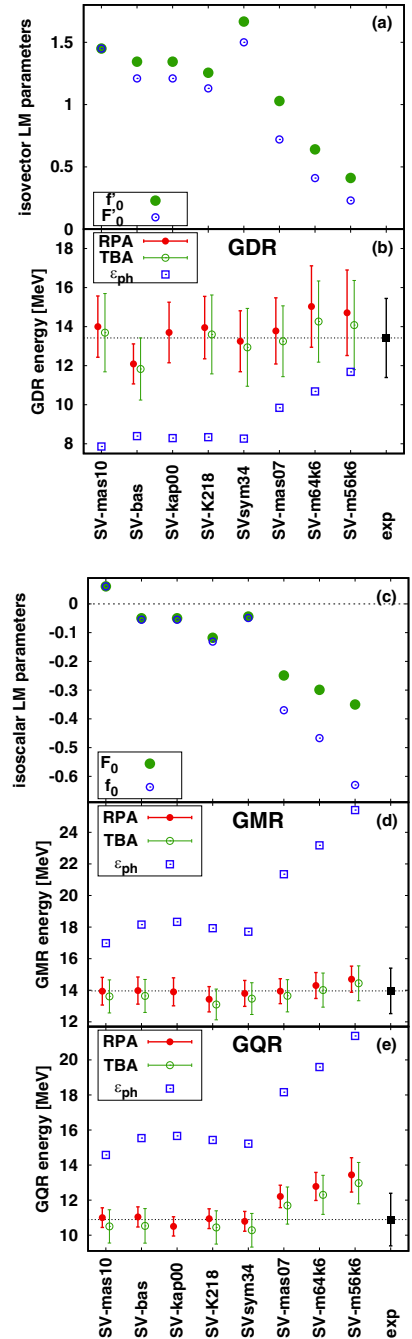


FIG. 2. Collection of giant-resonance properties in ^{208}Pb together with LM parameters for a representative set of Skyrme parametrizations covering a variation of all four NMP [16,44]. (a) Isovector LM parameters. (b) Isovector RPA properties (resonance energies, average 1ph energies). (c) Isoscalar LM parameters. (d) Isoscalar monopole resonance energies. (e) Isoscalar quadrupole resonance energies. In addition to RPA results, also results from TBA are shown and the unperturbed 1ph energies.

resonance (GQR) to the effective mass m^*/m . These trends are much more subtle than the dramatic trends for the ϵ_{ph} . It is remarkable how the interplay between mean-field and ph interaction can recover the subtle trends.

C. The magnetic case

In the case of magnetic modes, there are no isoscalar spin-dependent resonances known, which suggests that the spin-dependent isoscalar ph interaction is weak. On the other hand, there exist collective neutron-particle proton-hole resonances in nuclei with neutron excess. The best known resonances are the (1^+) Gamow-Teller resonances. The corresponding unperturbed 1ph-strength is shifted to higher energies, which is a clear indication that the spin-isospin ph interaction has to be strongly repulsive, which was confirmed in Ref. [50] comparing the experimental GT resonance in ^{208}Pb together with two theoretical results. However, the Gamow-Teller resonances reside in a regime where effective energy functionals are most probably insufficient. We thus concentrate on the low-energy magnetic modes. We have scanned several multiplicities and find that the $M1$ mode provides the cleanest test case for comparison with data while all other modes are more fragmented thus less suitable; for details see Appendix C. We thus concentrate here on $M1$ modes.

The 1^+ states in ^{208}Pb are a nice example of the behavior of the spin-dependent isoscalar and isovector interaction. There is an isoscalar state at $E_1 = 5.84$ MeV which is close to the uncorrelated (experimental) proton and neutron spin-orbit doublets $\epsilon_{\text{ph}}^{\pi} = 5.55$ MeV and $\epsilon_{\text{ph}}^{\nu} = 5.84$ MeV and a couple of isovector 1^+ states with the mean energy $E_2 = 7.39$ MeV. This again shows that the spin-dependent isoscalar ph interaction is weak and the spin-dependent isovector ph interaction is strongly repulsive. In a recent publication by our group [28], we investigated these 1^+ states in the framework of RPA using various Skyrme parameter sets with different effective masses. There we took the Skyrme functional as derived from a Skyrme interaction with all spin terms fixed by the model, option 2 of Sec. III C. Figure 3 shows the RPA results of the isoscalar and isovector $M1$ modes together with the unperturbed 1ph energies. The trends of the 1ph energies are the same as for the giant resonances in Fig. 2 and the computed $M1$ energies amplify this trend, driving the RPA results far off the experimental values. This demonstrates on the grounds of the empirical results that the option to take the Skyrme interaction literally is inappropriate for magnetic modes. In our paper [28], we also considered the spin terms in the Skyrme EDF as free for independent calibration (option 3 in Sec. III C). The energies of the $M1$ modes reproduce, by construction, the experimental energies and are thus not shown in the figure. The nontrivial message in this respect is that one can do such fine tuning of spin modes without destroying the overall quality of the parametrization.

V. CONCLUSION

Using a self-consistent, microscopic description based on an energy-density functional (EDF), we calculated collective low- and high-lying resonances for several Skyrme parametrizations with different effective masses. The electric resonances are in good agreement with the data whereas the magnetic resonances fail. This result, also found previously by other authors, is at first glance surprising because changing

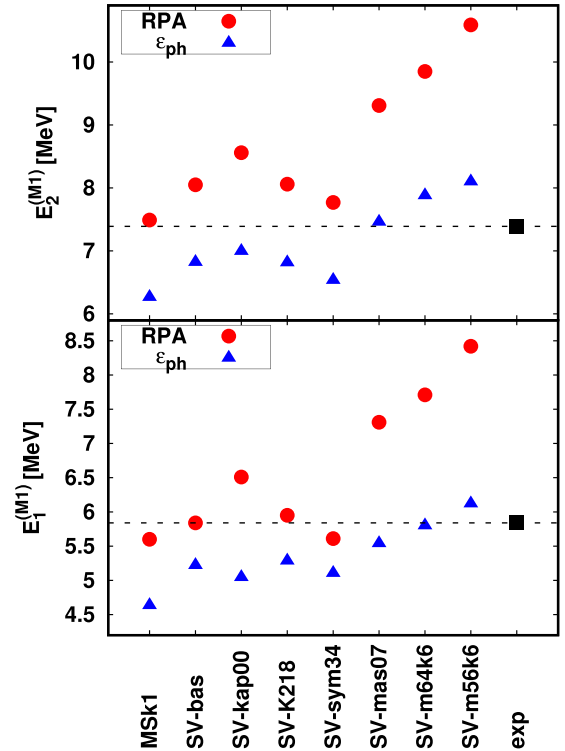


FIG. 3. Energies of the lower ($E_1^{(M1)}$, lower figure) and higher ($E_2^{(M1)}$, upper figure) $M1$ states in ^{208}Pb calculated within RPA for a selection of different Skyrme parametrizations (full red circle) compared with the experimental values (black box and faint dashed line). Also shown are the energy of the unperturbed ϵ_{ph} from proton spin-orbit pair (lower figure) and neutron spin orbit pair (upper figure), indicated by blue triangles.

the effective mass changes energy spacing of particle-hole (ph) states dramatically while, e.g., monopole resonances stay inert. The fact that giant resonances do not change that much requires that the change in ph spacing is compensated by a corresponding change in the residual ph interaction: smaller effective mass gives larger ph spacings and thus the ph interaction has to be more attractive (isoscalar channel) or less repulsive (isovector channel). Using the Landau-Migdal (LM) theory of fermion fluid, we could assess the mechanisms beyond this correlation between ph spacing and strength of residual ph interaction for the actual Skyrme EDFs. The volume parameters of the latter were quantified in terms of LM parameters which depend, apart from effective mass m^*/m , only on five nuclear matter parameters (Fermi momentum k_F , bulk binding energy B/A , incompressibility K_∞ , symmetry energy a_{sym} , and Thomas-Reiche-Kuhn sum rule enhancement κ_{TRK}). The LM theory shows that the LM parameters for natural-parity modes are constrained by basic conservation laws (continuity equation), a mechanism also known as backflow effect. These constraints do not apply in the unnatural-parity channel. These simple fluid dynamical considerations show that the spin parameters in a Skyrme EDF are, in principle, independent of the parameters for the natural-parity channel. If a Skyrme force establishes a relation between natural- and unnatural-parity channels, failure

is likely and that is what one finds in microscopic calculations.

Then we looked at magnetic modes, i.e., excitations with unnatural parity, in more detail. First of all, there exist no well settled magnetic bulk properties which may be included in the fitting of the EDF parameters. This leaves several options for determining the EDF in the spin channel. Either one derives the spin parameters from the zero-range Skyrme force as done traditionally, or one dismisses all terms which are not required by Galilean invariance, or one takes spin-sensitive data to calibrate them. Our results show that only the last option can work. However, there are no strong collective magnetic resonances known which could serve as a strong benchmark. An exception may be the GT resonances in neutron-rich nuclei which, unfortunately, are likely to lie outside the range of a description by Skyrme EDFs. Thus we take as reference here the strongest isoscalar and isovector $M1$ states in ^{208}Pb . The isoscalar state is close to the two (experimental) spin-orbit partners while the more fragmented isovector states are shifted by about 2 MeV to higher energies. Taking the definition of spin parameters in the EDF from the Skyrme force runs into difficulties for $M1$ resonances in ^{208}Pb . The RPA results do not describe the data and there do not exist the clear correlations between unperturbed ph states and RPA results like in the electric case. The main point of our paper is that this problem is already apparent from bulk properties, namely looking at the trends of the spin-dependent LM parameters g_0 and g'_0 as function of m^*/m . These trends are going in the opposite direction compared to the well performing LM parameters f_0 and f'_0 in the natural-parity channel. This provides, already at the level of bulk properties, a strong argument against the definition of a Skyrme EDF by a Skyrme force. The argument is corroborated by the observation that the values of g_0 and g'_0 differ substantially from those obtained previously by a fit to the empirical $M1$ resonances.

This altogether demonstrates, once again, that the spin channel in Skyrme EDF's is different and still requires careful calibration. The next step of development is to explore the chances to obtain a consistent description of spin properties (magnetic modes, properties of odd nuclei) by freely fitting the spin parameters of the Skyrme EDF. In that context, one should also consider the tensor spin-orbit terms in the EDF. In a further step, one should look at relativistic EDFs. These have spin properties inherently coupled to the natural-parity channel. The intriguing question is whether this gives at once a better description of the magnetic channel or whether one needs comparable extensions of the model (tensor couplings) to obtain a pertinent description.

ACKNOWLEDGMENT

This research was carried out using computational resources provided by the Computer Center of St. Petersburg State University.

APPENDIX A: DENSITY DEPENDENCE OF LM PARAMETERS

As mentioned above, the LM theory for finite nuclei as well as the SHF model augment the LM parameters with some

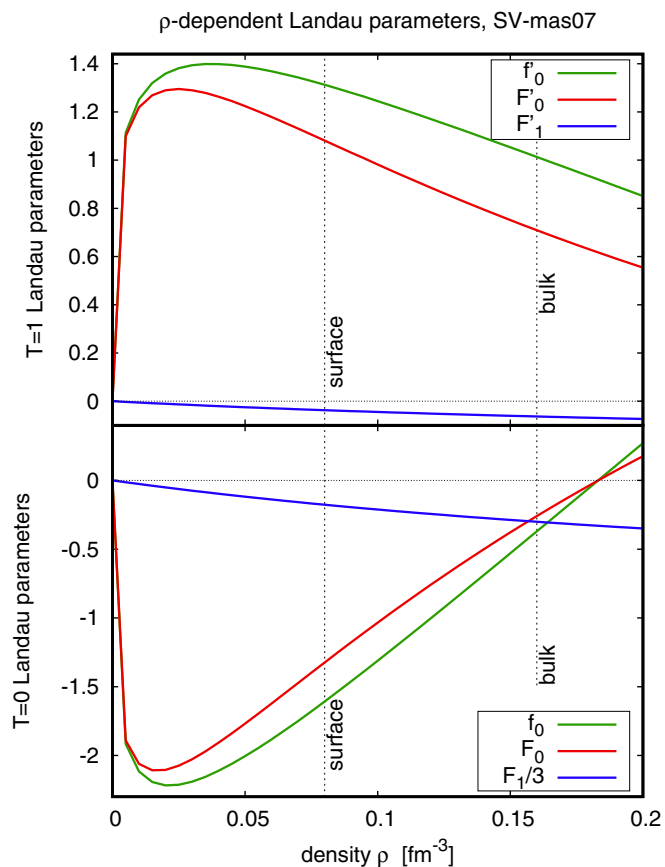


FIG. 4. Density dependence of the isovector LM parameters f'_0 , F'_0 , F'_1 in the upper part and the isoscalar LM parameters f_0 , F_0 , F_1 in the lower part. The quantities are derived from the Skyrme parametrization SV-mas07.

density dependence. Figure 4 shows the density-dependent LM parameters for the parametrization SV-mas07. Near bulk density, it is linear similar to LM theory. But it differs dramatically from linear behavior at low densities.

APPENDIX B: LOW-LYING COLLECTIVE ELECTRIC STATES

In Fig. 5 we present the energies of the first 3^- , 5^- , and 2^+ states in ^{208}Pb calculated in RPA with various Skyrme parametrizations. For each parameter set, also the energy of the lowest unperturbed 1ph state in the corresponding channel is given. From numberless calculations, e.g., Ref. [23], we know that the lowest 3^- state is the most collective state in ^{208}Pb . Many 1ph state within the $1\hbar\omega$ shell contribute coherently, which gives rise to the well known large transition probability and large energy shift. This is nicely demonstrated in panel (b) of Fig. 5, where all 1ph energies stay far above the final lowest state (red dots). To the 5^- state [panel (a)] also many 1ph states within the $1\hbar\omega$ shell contribute, but obviously in this case the ph interaction is too weak to generate a strongly collective state. Therefore the shift from the unperturbed states is much smaller and reaches in no case the experimental line. For the 2^+ states [panel (c)] only two

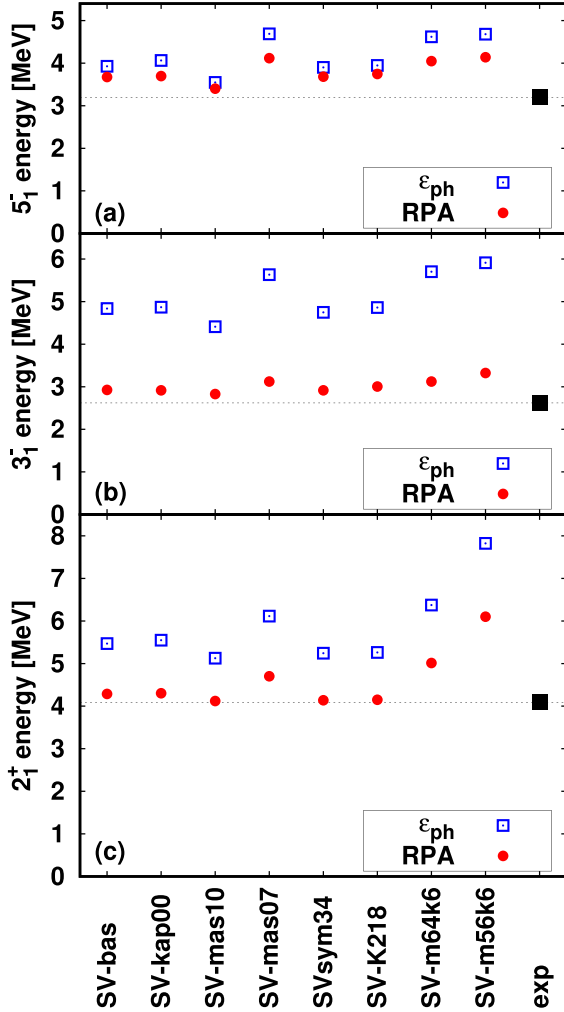


FIG. 5. Energies of the first excited 3^- , 5^- , and 2^+ states in ^{208}Pb calculated within RPA. We compare the results of different Skyrme parametrizations with the data. We also show the energy of the lowest unperturbed 1ph pair for each multipolarity, indicated by blue squares.

neutron and two proton 1ph states within the $1\hbar\omega$ shell contribute. On the other hand many 1ph states from the $2\hbar\omega$ shell contribute and give rise to a relatively large transition moment. The energy shifts are smaller than in the 3^- case, but reach in most cases the experimental value. The down-shift of the energy comes along with an enhanced transition moment (not shown here) which is another realization of collectivity (coherent superposition of many 1ph states). The most collective resonance in that respect is the 3^- state and it is no surprise that we see, again, the same feature as for the giant resonances, namely that the uncoupled 1ph energies change with Skyrme force while the RPA results are practically the same. From this we conclude that for collective states the *backflow* is an important corrective mechanism.

APPENDIX C: MAGNETIC MODES WITH $L = 1-6$

In the main part of our paper we discussed $M1$ modes only. For completeness, we show in Fig. 6 the spectral distributions

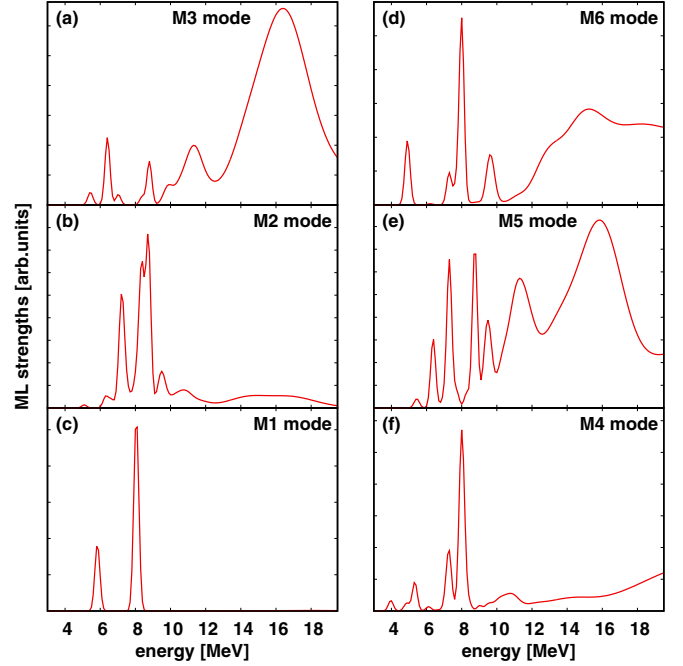


FIG. 6. Spectral distributions of ML strengths for the modes with $L = 1-6$ in ^{208}Pb computed with RPA using the Skyrme parametrization SV-bas [16]. The discrete RPA spectra are smoothed with Gaussians using energy-dependent width $\Gamma = \max(0.2, (E - 8)/5)$ MeV to simulate continuum effects and collision broadening.

of magnetic modes with angular momenta $L = 1-6$ in ^{208}Pb computed within the RPA using the Skyrme parametrization SV-bas. The external field operators of the magnetic excitations were taken in standard form; see, e.g., Ref. [9]. As demonstrated in Fig. 6, $M1$ excitations have by far the cleanest structure, with two pronounced and well separated low-lying structures. The lower one is of isoscalar nature and the higher states have isovector character. Moreover, there exist high-precision data for the $M1$ states. For this reason we used the $M1$ mode as tool for studying the spin properties of the ph interaction.

APPENDIX D: NUCLEAR MATTER PROPERTIES

Within the density functional theory, the properties of symmetric infinite nuclear matter (the Fermi momentum k_F , the total binding energy per nucleon B/A , the nuclear matter incompressibility K_∞ , the symmetry energy a_{sym} , the enhancement factor of the Thomas-Reiche-Kuhn sum rule κ_{TRK} , and the effective mass m^*) are determined by the parameters of the energy-density functional. In the case of Skyrme EDF (3) the respective equations have the following form (see, e.g., Ref. [51]):

$$0 = \frac{2}{5}T_F + \frac{3}{8}t_0\rho_{\text{eq}} + \frac{1}{16}t_3(\alpha + 1)\rho_{\text{eq}}^{\alpha+1} + \frac{1}{16}\Theta_s k_F^2 \rho_{\text{eq}}, \quad (\text{D1})$$

$$-B/A = \frac{3}{5}T_F + \frac{3}{8}t_0\rho_{\text{eq}} + \frac{1}{16}t_3\rho_{\text{eq}}^{\alpha+1} + \frac{3}{80}\Theta_s k_F^2 \rho_{\text{eq}}, \quad (\text{D2})$$

$$K_{\infty} = \frac{6}{5}T_F + \frac{9}{4}t_0\rho_{\text{eq}} + \frac{3}{16}t_3(\alpha + 1)(3\alpha + 2)\rho_{\text{eq}}^{\alpha+1} + \frac{3}{4}\Theta_s k_F^2 \rho_{\text{eq}}, \quad (\text{D3})$$

$$a_{\text{sym}} = \frac{1}{3}T_F - \frac{1}{8}t_0(2x_0 + 1)\rho_{\text{eq}} - \frac{1}{48}t_3(2x_3 + 1)\rho_{\text{eq}}^{\alpha+1} + \frac{1}{24}(2\Theta_s - 3\Theta_v)k_F^2 \rho_{\text{eq}}, \quad (\text{D4})$$

$$\kappa_{\text{TRK}} = \frac{m\rho_{\text{eq}}}{4\hbar^2}\Theta_v, \quad (\text{D5})$$

$$\frac{m}{m^*} = 1 + \frac{m\rho_{\text{eq}}}{8\hbar^2}\Theta_s, \quad (\text{D6})$$

where $\rho_{\text{eq}} = 2k_F^3/3\pi^2$ is the equilibrium density, $T_F = \hbar^2 k_F^2/2m$,

$$\Theta_s = 3t_1 + (5 + 4x_2)t_2, \quad (\text{D7})$$

$$\Theta_v = (2 + x_1)t_1 + (2 + x_2)t_2. \quad (\text{D8})$$

APPENDIX E: LANDAU-MIGDAL PARAMETERS

The Landau-Migdal parameters deduced from the Skyrme EDF (3) are related with the parameters of this functional by the formulas (see, e.g., Refs. [22,52])

$$C_0^* F_0 = \frac{3}{4}t_0 + \frac{1}{16}t_3(\alpha + 1)(\alpha + 2)\rho_{\text{eq}}^{\alpha} + \frac{1}{8}k_F^2[3t_1 + (5 + 4x_2)t_2], \quad (\text{E1})$$

$$C_0^* F'_0 = -\frac{1}{4}t_0(1 + 2x_0) - \frac{1}{24}t_3(1 + 2x_3)\rho_{\text{eq}}^{\alpha} + \frac{1}{8}k_F^2[(1 + 2x_2)t_2 - (1 + 2x_1)t_1], \quad (\text{E2})$$

$$C_0^* F_1 = -\frac{1}{8}k_F^2[3t_1 + (5 + 4x_2)t_2], \quad (\text{E3})$$

$$C_0^* F'_1 = -\frac{1}{8}k_F^2[(1 + 2x_2)t_2 - (1 + 2x_1)t_1], \quad (\text{E4})$$

$$C_0^*(G_0 + G_1) = -\frac{1}{4}t_0(1 - 2x_0) - \frac{1}{24}t_3(1 - 2x_3)\rho_{\text{eq}}^{\alpha}, \quad (\text{E5})$$

$$C_0^*(G'_0 + G'_1) = -\frac{1}{4}t_0 - \frac{1}{24}t_3\rho_{\text{eq}}^{\alpha}, \quad (\text{E6})$$

$$C_0^* G_1 = \frac{1}{8}[(1 - 2x_1)t_1 - (1 + 2x_2)t_2]k_F^2, \quad (\text{E7})$$

$$C_0^* G'_1 = \frac{1}{8}(t_1 - t_2)k_F^2, \quad (\text{E8})$$

with C_0^* as defined in Eq. (5b). Note that $G_1 = G'_1 = 0$ independently of Eqs. (E7) and (E8) for the Skyrme EDFs in which the \mathbf{J}^2 terms are omitted (see Ref. [53] for more detail).

-
- [1] M. Bender, P.-H. Heenen, and P.-G. Reinhard, *Rev. Mod. Phys.* **75**, 121 (2003).
- [2] P. Vesely, J. Kvasil, V. O. Nesterenko, W. Kleinig, P.-G. Reinhard, and V. Y. Ponomarev, *Phys. Rev. C* **80**, 031302(R) (2009).
- [3] V. O. Nesterenko, J. Kvasil, P. Vesely, W. Kleinig, P.-G. Reinhard, and V. Y. Ponomarev, *J. Phys. G: Nucl. Part. Phys.* **37**, 064034 (2010).
- [4] A. B. Migdal, *Theory of Finite Fermi Systems and Application to Atomic Nuclei* (Wiley, New York, 1967).
- [5] L. D. Landau, E. M. Lifshitz, and L. P. Pitaevskii, *Course of Theoretical Physics 9—Statistical Physics* (Pergamon, Oxford, 1980).
- [6] P. Ring and P. Schuck, *The Nuclear Many-Body Problem* (Springer, New York, 1980).
- [7] V. I. Tselyaev, *Phys. Rev. C* **75**, 024306 (2007).
- [8] V. Tselyaev, N. Lyutorovich, J. Speth, S. Krewald, and P.-G. Reinhard, *Phys. Rev. C* **94**, 034306 (2016).
- [9] J. Speth, E. Werner, and W. Wild, *Phys. Rep.* **33**, 127 (1977).
- [10] T. H. R. Skyrme, *Nucl. Phys.* **9**, 615 (1959).
- [11] J. W. Negele and D. Vautherin, *Phys. Rev. C* **5**, 1472 (1972).
- [12] J. W. Negele and D. Vautherin, *Phys. Rev. C* **11**, 1031 (1975).
- [13] K. F. Liu and G. E. Brown, *Nucl. Phys. A* **265**, 385 (1976).
- [14] D. Vautherin and D. Brink, *Phys. Rev. C* **5**, 626 (1972).
- [15] J. Bartel, P. Quentin, M. Brack, C. Guet, and H.-B. Håkansson, *Nucl. Phys. A* **386**, 79 (1982).
- [16] P. Klüpfel, P.-G. Reinhard, T. J. Bürvenich, and J. A. Maruhn, *Phys. Rev. C* **79**, 034310 (2009).
- [17] J. Erler and P.-G. Reinhard, *J. Phys. G* **42**, 034026 (2014).
- [18] J. Bardin and J. R. Schrieffer, in *Progress in Low Temperature Physics*, Vol. 3, edited by C. J. Gorter (North-Holland, Amsterdam, 1961), p. 170.
- [19] G. F. Bertsch and S. F. Tsai, *Phys. Rep.* **18**, 125 (1975).
- [20] H. Krivine, J. Treiner, and O. Bohigas, *Nucl. Phys. A* **336**, 155 (1980).
- [21] J. S. Bell and T. H. R. Skyrme, *Philos. Mag.* **1**, 1055 (1956).
- [22] N. Van Giai and H. Sagawa, *Phys. Lett. B* **106**, 379 (1981).
- [23] P. Ring and J. Speth, *Phys. Lett. B* **44**, 477 (1973).
- [24] J. Speth, V. Klemt, J. Wambach, and G. E. Brown, *Nucl. Phys. A* **343**, 382 (1980).
- [25] E. Migli, S. Drożdż, J. Speth, and J. Wambach, *Z. Phys. A* **340**, 111 (1991).
- [26] P. Sarriguren, E. Moya de Guerra, and R. Nojarov, *Z. Phys. A* **357**, 143 (1997).
- [27] S. Goriely, S. Hilaire, S. Péru, M. Martini, I. Deloncle, and F. Lechaftois, *Phys. Rev. C* **94**, 044306 (2016).
- [28] V. Tselyaev, N. Lyutorovich, J. Speth, P.-G. Reinhard, and D. Smirnov, *Phys. Rev. C* **99**, 064329 (2019).
- [29] J. Speth and D. Zawischa, *Phys. Lett. B* **211**, 247 (1988).
- [30] J. Speth and D. Zawischa, *Phys. Lett. B* **219**, 529 (1989).
- [31] A. Faessler and R. Nojarov, *Phys. Rev. C* **41**, 1243 (1990).
- [32] D. Zawischa and J. Speth, *Phys. Lett. B* **252**, 4 (1990).
- [33] D. Zawischa, M. Macfarlane, and J. Speth, *Phys. Rev. C* **42**, 1461 (1990).
- [34] P. Sarriguren, E. Moya de Guerra, and R. Nojarov, *Phys. Rev. C* **54**, 690 (1996).
- [35] J. Erler, P. Klüpfel, and P. G. Reinhard, *J. Phys. G* **38**, 033101 (2011).

- [36] P.-G. Reinhard, *Ann. Phys. (Leipzig)* **504**, 632 (1992).
- [37] A. Repko and J. Kvasil, *Acta Phys. Pol. B Proc. Suppl.* **12**, 689 (2019).
- [38] D. Pines and P. Nozières, *The Theory of Quantum Liquids* (W. A. Benjamin, New York, 1966).
- [39] J. A. McNeil, R. D. Amado, C. J. Horowitz, M. Oka, J. R. Shepard, and D. A. Sparrow, *Phys. Rev. C* **34**, 746 (1986).
- [40] L. D. Landau, *Sov. Phys. JETP* **3**, 920 (1957).
- [41] L. D. Landau, *Sov. Phys. JETP* **5**, 101 (1957).
- [42] L. D. Landau, *Sov. Phys. JETP* **8**, 70 (1959).
- [43] J. Speth, S. Krewald, F. Grümmer, P. G. Reinhard, N. Lyutorovich, and V. Tselyaev, *Nucl. Phys. A* **928**, 17 (2014).
- [44] N. Lyutorovich, V. I. Tselyaev, J. Speth, S. Krewald, F. Grümmer, and P.-G. Reinhard, *Phys. Rev. Lett.* **109**, 092502 (2012).
- [45] P.-G. Reinhard, *Rep. Prog. Phys.* **52**, 439 (1989).
- [46] K. J. Pototzky, J. Erler, P.-G. Reinhard, and V. O. Nesterenko, *Eur. Phys. J. A* **46**, 299 (2010).
- [47] J. Speth and J. Wambach, in *Electric and Magnetic Giant Resonances in Nuclei*, International Review of Nuclear Physics, Vol. 7, edited by J. Speth (World Scientific, Singapore, 1991), pp. 2–87.
- [48] V. Tselyaev, N. Lyutorovich, J. Speth, and P.-G. Reinhard, *Phys. Rev. C* **96**, 024312 (2017).
- [49] V. Tselyaev, N. Lyutorovich, J. Speth, and P.-G. Reinhard, *Phys. Rev. C* **97**, 044308 (2018).
- [50] T. Wakasa, M. Okamoto, M. Dozono, K. Hatanaka, M. Ichimura, S. Kuroita, Y. Maeda, H. Miyasako, T. Noro, T. Saito, Y. Sakemi, T. Yabe, and K. Yako, *Phys. Rev. C* **85**, 064606 (2012).
- [51] E. Chabanat, P. Bonche, P. Haensel, J. Meyer, and R. Schaeffer, *Nucl. Phys. A* **627**, 710 (1997).
- [52] J. Margueron, J. Navarro, and N. V. Giai, *Phys. Rev. C* **66**, 014303 (2002).
- [53] T. Lesinski, M. Bender, K. Bennaceur, T. Duguet, and J. Meyer, *Phys. Rev. C* **76**, 014312 (2007).